Horizontal-Longitudinal Correlations of Acoustic Field in Deep Water *

LI Jun(李鋆)[1,2], LI Zheng-Lin(李整林)[1,3**], REN Yun(任云)[1], LI Wen(李文)[1,2], ZHANG Ren-He(张仁和)[1]

[1]*State Key Laboratory of Acoustics, Institute of Acoustics, Chinese Academy of Sciences, Beijing 100190*

[2]*University of Chinese Academy of Sciences, Beijing 100190*

[3]*Haikou Laboratory of Acoustics, Institute of Acoustics, Chinese Academy of Sciences, Haikou 570105*

(Received 9 February 2015)

The horizontal-longitudinal correlations of the acoustic field in deep water are investigated based on the experimental data obtained in the South China Sea. It is shown that the horizontal-longitudinal correlation coefficients in the convergence zone are high, and the correlation length is consistent with the convergence zone width, which depends on the receiver depth and range. The horizontal-longitudinal correlation coefficients in the convergence zone also have a division structure for the deeper receiver. The signals from the second part of the convergence zone are still correlated with the reference signal in the first part. The horizontal-longitudinal correlation coefficients in the shadow zone are lower than that in the convergence zone, and the correlation length in the shadow zone is also much shorter than that in the convergence zone. The numerical simulation results by using the normal modes theory are qualitatively consistent with the experimental results.

PACS: 43.30.Bp, 43.30.Re DOI: 10.1088/0256-307X/32/6/064303

With the development of sonar applications and the large acoustic array-processing technique, studying the horizontal-longitudinal correlations of the acoustic field, which is the physical foundation, is becoming more and more important.[1] Many works have been carried out on the horizontal-longitudinal correlations in shallow water in the past few years.[1−5] Su *et al.* analyzed and interpreted the oscillation pattern and strong fluctuations of the horizontal-longitudinal correlations using the normal modes interference theory in shallow water.[2] Wan *et al.* came to the conclusion that the longitudinal horizontal coherence length in units of wavelength increases with the range and frequency when the source and the receivers are below the thermocline in shallow water.[3] Li *et al.* observed the same phenomenon and indicated that the non-linear frequency relationship of the bottom attenuation is the main cause of this phenomenon.[5]

Recently, research interest has focused on the acoustic field in deep water. The characteristics of convergence zones in deep water waveguides can be used in long distance detection. Colosi *et al.* calculated the horizontal coherence using both the quadratic transport theory and quadratic adiabatic approximation simulations based on a deep-water Philippine Sea environment, obtained that the coherence length at the 500 km range is 1900 m when using the $e^{-1/2}$ decay of the normalized depth average coherence, the range scaling is precisely $R^{-1/2}$, and the frequency scaling is very close to $f^{-1.12}$.[6] The interference patterns in the convergence zones and shadow zones are very different in deep water.[7] Therefore, the empirical relationship of the horizontal-longitudinal coherence length in convergence zones and shadow zones should not be the same as those in Ref. [6].

The purpose of this work is to analyze the horizontal-longitudinal correlations in the convergence zone and the shadow zone based on the experimental data obtained in the South China Sea. The experimental results show that the horizontal-longitudinal correlation length in the convergence zone is much longer than that in the shadow zone. These new results provide a foundation for future research of horizontal-longitudinal correlations and sonar applications in deep water.

Under the condition that sound speed and density depend only on depth z, the underwater acoustic pressure field generated by a point source can be expressed by the normal modes theory; the sound pressure can be written as[8]

$$p(r,z) \approx \frac{i}{\rho(z_s)\sqrt{8\pi r}} e^{-i\pi/4} \sum_{m=1}^{\infty} \Psi_m(z_s)\Psi_m(z)\frac{e^{ik_{rm}r}}{\sqrt{k_{rm}}}, \quad (1)$$

where $\Psi_m(z_s)$ and $\Psi_m(z)$ are the eigenfunctions at the source and the receiver, respectively, k_{rm} is the horizontal wavenumber of the mth mode.

The horizontal-longitudinal correlation coefficient is defined as the normalized cross correlation between the two separated points' sound pressures received at the same depth. It describes the similarity of the acoustic fields at two separated points. If $p_r(t)$ and $p_{r+\Delta r}(t)$ are the sound pressures received at the two positions (r, z_r) and $(r+\Delta r, z_r)$, the horizontal-longitudinal correlation coefficient can be expressed as

$$\rho(r, r+\Delta r) = \max_{\tau} \frac{\int_{-\infty}^{\infty} p_r(t) p_{r+\Delta r}(t+\tau) dt}{\sqrt{\int_{-\infty}^{\infty} p_r^2(t) dt \int_{-\infty}^{\infty} p_{r+\Delta r}^2(t) dt}}, \quad (2)$$

where τ is the time delay, and Δr is the longitudinal separation satisfying $\Delta r \ll r$. The expression in the frequency domain can be written as

$$\rho(\Delta r) = \max_{\tau} \frac{Re[\int_{\omega_1}^{\omega_2} P_r(\omega) P_{r+\Delta r}^*(\omega) e^{i\omega\tau} d\omega)]}{\sqrt{\int_{\omega_1}^{\omega_2} |P_r(\omega)|^2 d\omega \int_{\omega_1}^{\omega_2} |P_{r+\Delta r}(\omega)|^2 d\omega}}, \quad (3)$$

*Supported by the National Natural Science Foundation of China under Grant Nos 11434012 and 11174312.

**Corresponding author. Email: lzhl@mail.ioa.ac.cn

where $P_r(\omega)$ and $P_r + \Delta r(\omega)$ are the spectra of $p_r(t)$ and $p_{r+\Delta r}(t)$, $*$ represents the complex conjugation, ω denotes the angular frequency, and ω_1 and ω_2 are the lower and upper angular frequencies of the emitted signals, respectively.

Equation (2) is used to calculate the correlation coefficient in the following experimental data analysis, and Eqs. (1) and (3) are used in the numerical simulation. The horizontal-longitudinal correlation length is defined as the longitudinal separation when the correlation coefficient decays to $\sqrt{2}/2$.

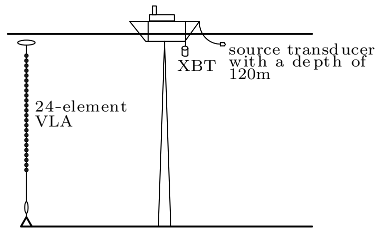

Fig. 1. Experimental configuration.

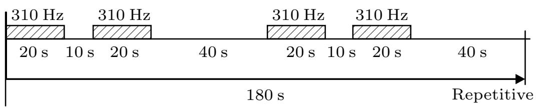

Fig. 2. The time series of the transmitted LFM signals from 260 Hz to 360 Hz.

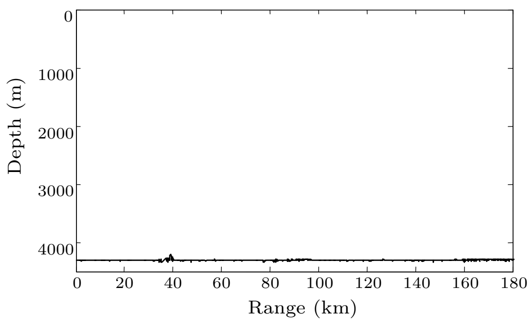

Fig. 3. Water depth along the propagation track.

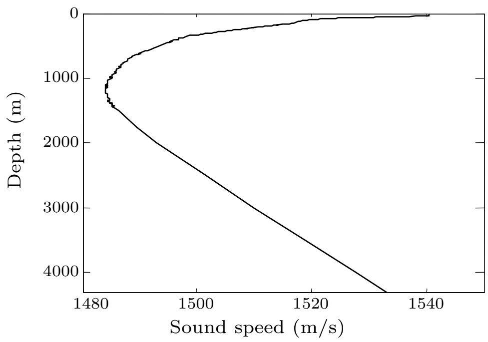

Fig. 4. Sound speed profile measured in the experimental site.

To study the horizontal-longitudinal correlations of the acoustic field in deep water, an experiment was conducted in the South China Sea in October 2013. As shown in Fig. 1, the receiving array was a 24-element vertical line array (VLA) fixed at a location with the depth from 143 m to 1852 m. The transducer source was towed from the Chinese R/V Shi Yan 1 from the Institute of Acoustics, Chinese Academy of Sciences towards the receiving array with the depth at 120 m at a speed of 4 knot. The linear frequency module (LFM) signals from 260 Hz to 360 Hz with a duration of 20 s were transmitted twice every 90 s, as shown in Fig. 2. The nominal maximum source level at the transducer resonance (about 310 Hz) was 184.2 dB at 1 μPa@1 m. The maximal propagation range was about 180 km containing three convergence zones. The water depth along the propagation track is shown in Fig. 3. It is nearly a flat bottom with the mean depth of 4305 m. Figure 4 shows the sound speed profile measured by using CTD cast near the receiver array. The sound channel axis depth is about 1164 m with a sound speed of 1483.97 m/s, and the sound speed near the bottom is 1533 m/s. The bottom sediment is core sampled in this experiment, and the results show that the surface bottom sediment type is silty clay with the density of 1.6 g/cm^3.

The original LFM signals from the transducer are denoted as $s(t)$. The received signal from one element of the VLA can be expressed as

$$s_R(t) = \int S(\omega)P(r, z; \omega)\exp(-i\omega t)d\omega, \qquad (4)$$

where $S(\omega)$ is the spectrum of $s(t)$, and $P(r, z; \omega)$ is the transfer function of the ocean environment from source to receiver. The pulse compression technique, which correlates $s(t)$ with $s_R(t)$, is used to increase the signal-to-noise ratio (SNR). The compressed signal can be expressed as

$$s_{\rm C}(t) = \int |S(\omega)|^2 P(r, z; \omega)\exp(-i\omega t)d\omega. \qquad (5)$$

In fact, $s_{\rm C}(t)$ is the received signal of the autocorrelation function of $S(\omega)$ propagating through the deep ocean channel $P(r, z; \omega)$.

From the compressed pulse signals by using Eq. (5), the transmission loss (TL) in different ranges and depths can be derived, as shown in Fig. 5. For comparison, the numerical narrow band TL at two different typical receiver depths are calculated from the normal mode program KrakenC,[8,9] as shown in Fig. 6. In the simulation, the two-layer equivalent bottom model is used. The sediment layer has a thickness of 5 m, a sound speed of 1565 m/s, a density of 1.6 g/cm^3, and the attenuation coefficient is 0.09 dB/m. The infinite basement has a sound speed of 1650 m/s, a density of 1.8 g/cm^3, and an attenuation coefficient of $0.4f^{0.9}$ dB/m[10], where f is in units of kHz. It can be seen from Figs. 5 and 6 that the location and width of the convergence zone vary with depth. Each convergence zone includes two sound beams with higher intensity in the range for a deeper receiver caused by refraction in the deep water sound channel. In Fig. 6(a), the first convergence zone covers the range from 51 km to 58 km at depth 167 m. In Fig. 6(b), the first convergence zone is with the first part from 42.5 km to 48.5 km, and the second part from 61.5 km to 64.5 km at a deeper depth of 1852 m. Figure 6 shows that the experimental TLs are in good agreement with the numerical ones. Therefore, the two-layer bottom model is applicable for the sea area of our experiment.

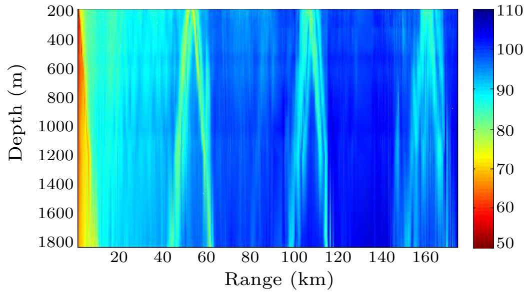

Fig. 5. Transmission losses of the experiment in different ranges and depths.

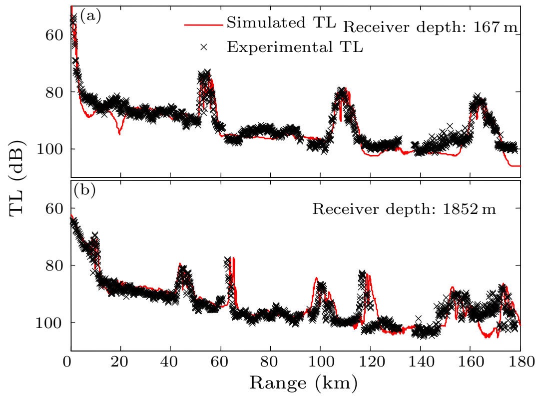

Fig. 6. Comparison of simulation/experiment transmission loss where the receiver depths are at 167 m and 1852 m, respectively.

According to Eq. (2), the compressed pulse signals are used to analyze the horizontal-longitudinal correlations of an acoustic field in deep water. The numerical horizontal-longitudinal correlation coefficient is obtained by substituting the simulated pressures into Eq. (3). Figure 7 shows the comparison of simulated and experimental horizontal-longitudinal correlation coefficient as a function of longitudinal separation in three convergence zones, where the receiver depth is 167 m. In Fig. 7(a), the red solid line and the circles depict the simulated and experimental horizontal-longitudinal correlation coefficients, respectively, in the reference range of 51.6 km which represents the first convergence zone. It is shown that the correlation length is about 6.5 km. Figures 7(b) and 7(c) show the results of the second and the third convergence zones, respectively. The correlation length is about 10 km. Comparing Fig. 6(a) with Fig. 7, we can conclude that the horizontal-longitudinal correlation coefficients in the convergence zone are high and the correlation length is consistent with the convergence zone width. The horizontal-longitudinal correlation coefficients in the third convergence zone are higher than those in the first and second convergence zones, as shown in Fig. 7. Due to the mode stripping, the number of effective propagating modes decreases with the increasing range. What is more, the energy of surface and bottom reflection also reduces with the increasing range. This, in turn, enhances the horizontal-longitudinal correlation.

For the deeper receiver, we select the maximal longitudinal separation as 26 km to cover the two parts of the convergence zone in data analysis. Figure 8 shows the comparison of the simulated and experimental horizontal-longitudinal correlation coefficients as a function of longitudinal separation in three convergence zones for the receiver depth at 1852 m. In the same TL data as shown in Fig. 6(b), the horizontal-longitudinal correlation coefficients in the convergence zone also have a division structure. This means that the signals from the second part of the convergence zone are still correlated with the reference signal in the first part.

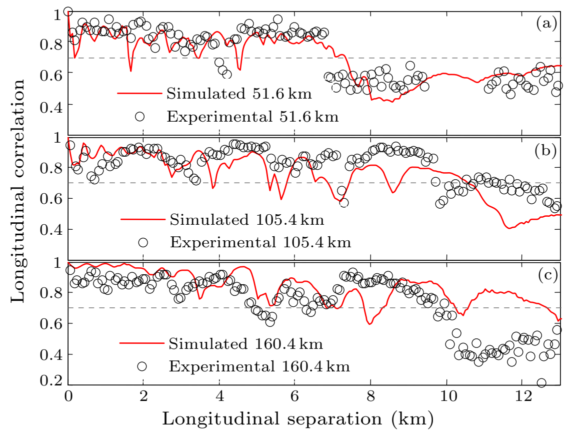

Fig. 7. Comparison of simulated/experimental horizontal-longitudinal correlations in (a) the first, (b) the second, and (c) the third convergence zones, where the receiver depth is 167 m.

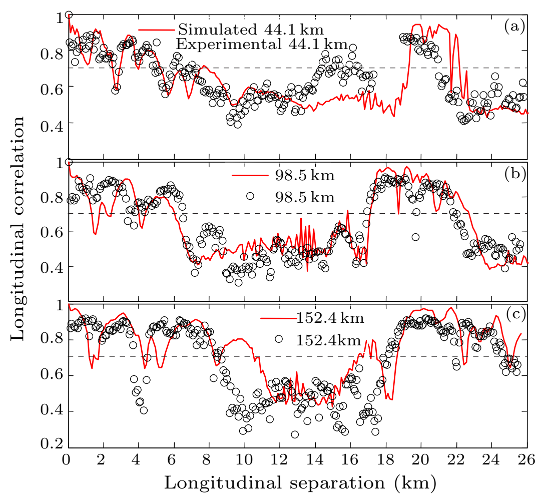

Fig. 8. Comparison of simulated/experimental horizontal-longitudinal correlations in (a) the first, (b) the second, and (c) the third convergence zones, where the receiver depth is 1852 m.

From Fig. 5, we can see that the acoustic field in the shadow zone does not have an obvious depth structure. Figure 9 shows the comparison of simulated and experimental horizontal-longitudinal correlation coefficients as a function of the longitudinal separation in three shadow zones, where the receiver depth is 167 m. In Fig. 9, the blue dashed line and the + depict the simulated and experimental horizontal-longitudinal correlation coefficients in the reference range of 26.9 km which represents the first shadow zone. Figures 9(b) and 9(c) show the results of the second and the third shadow zones, respectively. It is indicated that the horizontal-longitudinal correlation coefficients in the shadow zone are lower than those in the convergence zone and the correlation length in the shadow zone is also much shorter than that in the convergence zone.

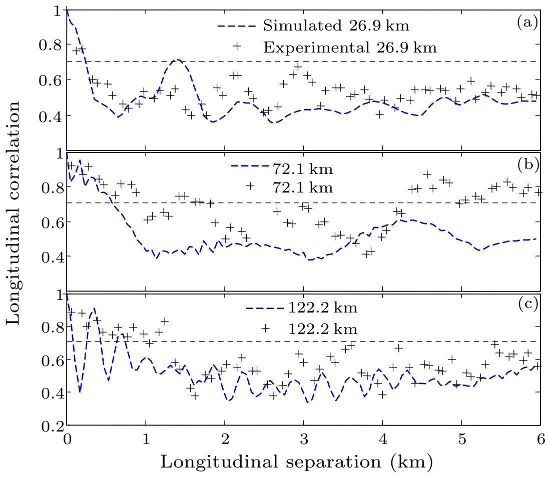

Fig. 9. Comparison of simulated/experimental horizontal-longitudinal correlations in (a) the first, (b) the second, and (c) the third shadow zones, where the receiver depth is 167 m.

Equation (3) in Ref. [2] indicates that the difference of the different-mode phase ($k_{rm}\Delta r$) causes the horizontal-longitudinal decorrelation. In general, in the deep waveguide the acoustic field in the convergence zone is mainly contributed from the waterborne modes, of which the phases are close and the signal structures are nearly the same. On the contrary, the acoustic field in the shadow zone is mainly contributed from the bottom bounce modes,[7] which has a similar frequency range interference pattern as in shallow water. This indicates that the influencing mechanism of the horizontal-longitudinal correlation length in the shadow zone is the same as that in shallow water. The correlation length in shallow water is approximately 10–20 acoustic wavelengths.[3] However, the cycle distance caused by bottom reflection increases with the water depth, and the correlation length in the shadow zone of deep water is about 40–200 acoustic wavelengths in this work.

From Figs. 7–9, it is seen that the correlation coefficients in both the convergence zone and the shadow zone oscillate and fluctuate apparently with the longitudinal separation. The fluctuation in the shadow zone is very complex at different depths or ranges. When the longitudinal separation Δr satisfies that the phases of the m_1th and the m_2th modes are opposite, the correlation coefficient will be minimal.[2]

In summary, the horizontal-longitudinal correlations of the acoustic field in deep water have been investigated based on the experimental data. Some conclusions can be drawn as follows: (i) the horizontal-longitudinal correlation coefficients in the convergence zone are high, and the correlation length is consistent with the convergence zone width, which depends on the receiver depth and range. The main cause of the phenomenon is that the energies in the convergence zone mainly come from a group of waterborne modes which have nearly similar phases. (ii) The same as in the TL data, the horizontal-longitudinal correlation coefficients in the convergence zone also have a division structure for the deeper receiver. The signals from the second part of the convergence zone are still correlated with the reference signal in the first part. (iii) The horizontal-longitudinal correlation coefficients in the shadow zone are lower than those in the convergence zone and the correlation length in the shadow zone is also much shorter than that in the convergence zone. The fluctuation of the horizontal-longitudinal correlation coefficients in the shadow zone is much more complex at different depths or ranges. The bottom bounce modes and the phase difference in the shadow zone are the main cause of this phenomenon.

We would like to express our great appreciation to all the researchers who participated in the experiment for their hard work.

References

[1] Guo L H, Gong Z X and Wu L X 2001 *Chin. Phys. Lett.* **18** 1366
[2] Su X X, Li F H and Jian S S 2007 *Tech. Acoust.* **26** 579 (in Chinese)
[3] Wan L et al 2009 *Acoust. Phys.* **55** 383
[4] Wang Q and Zhang R H 1992 *J. Acoust. Soc. Am.* **92** 932
[5] Li F H and Zhang R H 2008 *Chin. Phys. Lett.* **25** 2539
[6] Colosi J A and Chandrayadula T K 2013 *J. Acoust. Soc. Am.* **134** 3119
[7] Li Q Q, Li Z L and Zhang R H 2011 *Chin. Phys. Lett.* **28** 034303
[8] Jensen F B et al 2011 *Computational Ocean Acoustics* 2nd edn (New York: Springer)
[9] Li Z L, Zhang R H et al 2004 *Sci. Chin. G-Phys. Mech. Astron.* **47** 571
[10] Li Z L and Zhang R H 2004 *Chin. Phys. Lett.* **21** 1100